DEVELOPMENT OF ACCELERATOR SYSTEM AND BEAM DIAGNOSTIC INSTRUMENTS FOR NATURAL RUBBER AND POLYMER RESEARCH

E. Kongmon†, N. Kangrang, S. Rimjaem, J. Saisut, C. Thongbai, Plasma and Beam Physics Research Facility, Department of Physics and Materials Science, Faculty of Science, Chiang Mai University, Chiang Mai 50200, Thailand
M.W. Rhodes, Thailand Center of Excellence in Physics, Commission on Higher Education, Bangkok 10400, Thailand
P. Wichaisirimongkol, Science and Technology Research Institute, Chiang Mai University, Chiang Mai 50200, Thailand

Abstract

This research aims to design and develop an electron linear accelerator system and beam diagnostic instruments for natural rubber and polymer research at the Plasma and Beam Physics Research Facility, Chiang Mai University, Thailand. The accelerator consists of a DC thermionic electron gun and an S-band standing-wave linac. The system can produce electron beams with the energy range of 0.5 to 4 MeV for the pulse repetition rate of 30 to 200 Hz and the pulse duration of 4 μs. Commissioning of the accelerator system and development of beam diagnostic instruments to measure electron beam energy, electron pulse current and electron dose are underway. This contribution presents and discusses on the RF commissioning progress as well as status of design and construction of the beam diagnostic system.

INTRODUCTION

A linear accelerator (linac) system for electron beam irradiation on natural rubber and polymeric materials is developed at the Plasma and Beam Physics Research Facility, Chiang Mai University, Thailand. The system consists of a Pierce-type DC gun with a flat circular thermionic cathode with diameter of 4.86 mm, a 5-cell standing-wave linac structure equipped with a driven radio-frequency (RF) system, electron beam diagnostic instruments and an irradiation apparatus. It is foreseen that the irradiation system composes of a beam sweeper with a vacuum horn chamber and a movable stage for the sample container. The layout of the accelerator and irradiation system is shown in Fig. 1.

The electron beam diagnostic instruments are under design and construction. A Faraday cup and an integrated current transformer will be used to measure the electron charge and pulse current. A dipole magnet and phosphor screen equipped with a CCD camera readout system will be utilized for an electron beam energy measurement. The results from the current and energy measurement can be used to estimate the electron dose produced from the accelerator system. The transverse beam size and transverse electron distribution at the sample container location will be observed via an outside vacuum screen station. The electron depth and dose distribution will also be measured with dosimeter [1]. In this paper, we present the results of the RF commissioning, electron beam dynamic simulations and status of preparation for the beam diagnostic instruments.

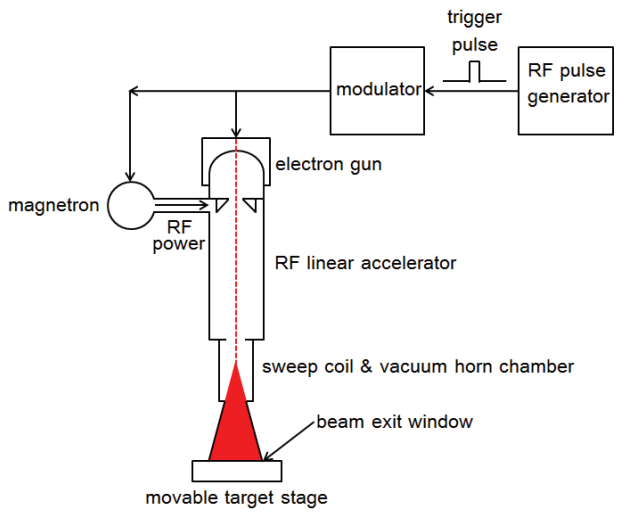

Figure 1: Layout of electron linear accelerator, a related RF power system and an irradiation apparatus.

HIGH POWER RF COMMISSIONING

The linac system can be used to accelerate electron beam to reach the average kinetic energy of 0.5 to 4 MeV depending on the supplied RF peak power, which can be varied from 0.66 to 2 MW. A diagram of the RF generator and measurement systems are shown in Fig.2. The main components of the RF generator are a high voltage power supply with a variac for voltage variable (VAC), a pulse forming network (PFN) and a pulse modulator system. The RF signal amplitude is generated and amplified by a magnetron to reach the MW level. Then, the RF wave is transported from the magnetron to the linac via a WR-284 rectangular waveguide system with a ceramic RF window to separate the SF_6 pressurized part and the vacuum part. A forward and reflected RF powers are measured at a directional coupler prior the ceramic RF window.

As shown in Fig. 2, the forward and reflected RF ports of the directional coupler have the attenuation values of -60 dB. The forward and reflected RF power ports are connected to the cables and the attenuators with total attenuation values of -96.66 dB and -97.89 dB, respectively. The RF signals are converted to analog

†Corresponding author: Ekkachai_kon@cmu.ac.th

ISBN 978-3-95450-177-9

Copyright © 2016 CC-BY-3.0 and by the respective authors

signals by using crystal detectors, which can be measured with a digital oscilloscope.

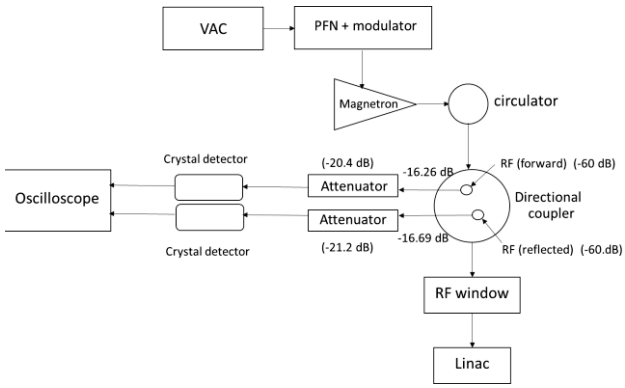

Figure 2: Schematic layout of the RF system.

During the RF commissioning, an operating temperature of 35°C, an RF pulse width of 4 μs and a current of the magnetron filament of 0.42 A were used. The variac (VAC) was adjusted from 70% to 85% with 5% for each step in order to vary the high voltage value and also the RF peak power. The result of this measurement in Fig. 3 shows that the RF peak power increases almost linearly from 0.9 MW to 2 MW for the high voltage value of 5 to 6.8 kV.

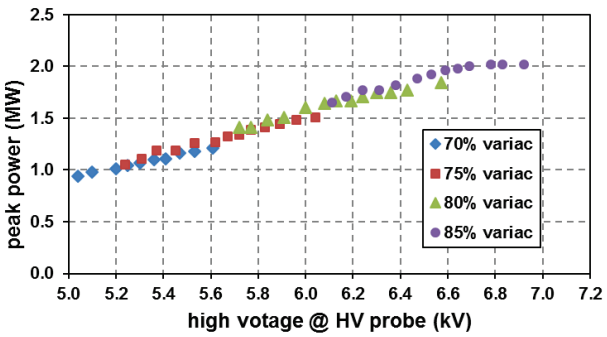

Figure 3: Relationship between the high voltage value and the peak power of the forward RF signal.

The average power of the RF wave can be calculated by using the following equation

$$P_{average} = (\tau)(pps)(P_{peak}), \quad (1)$$

where τ is the RF pulse width, which is equal to 4 μs. Here, pps is the pulse repetition rate, which was adjusted from 30 to 200 Hz in this experiment and P_{peak} is the RF peak power. The relationship between the pulse repetition rate and the average power for each variac level is shown in Fig. 4. An example of the measurement result of forward and reflected RF signals at the pulse repetition rate of 200 Hz are shown in Fig. 5. In this measurement, the forward peak power is 1.65 MW and the reflected RF power is 0.38 MW. Thus, the absorb RF power in this case is 1.27 MW. In the high power RF measurement, the resonant frequency of the linac structure was measured to be 2997.103 GHz, while the measured value for the low-power RF measurement with the S-parameter network analyser was 2996.816 MHz. The frequency difference of 187 kHz is probably due to the resolution of the frequency measurement with the spectrum analyzer in the high power measurement. The RF commissioning results are summarized in Table 1.

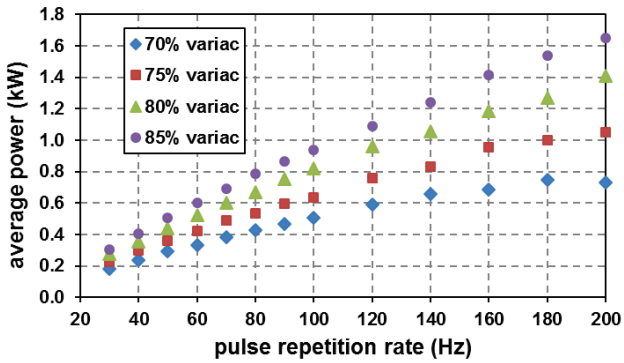

Figure 4: Relationship between the pulse repetition rate and the average power.

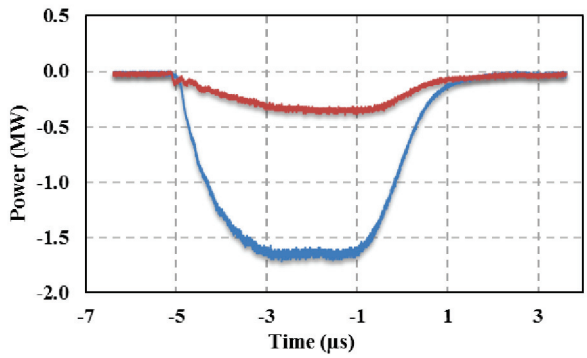

Figure 5: Forward (blue-line) and reflected (red-line) RF signals of 85% VAC at the pulse repetition rate of 200 Hz.

Table 1: Summary of RF Commissioning Results

Parameter	Value
Resonant frequency	2997.103 MHz
Resonant temperature	35°C
RF peak power	0.9 - 2 MW
Maximum pulse duration	4 μs
Pulse repetition rate	25-200 Hz

ELECTRON BEAM DYNAMIC STUDY

Electron beam dynamic study inside the linac structure was performed by using A Space Charge Tracking Algorithm ASTRA [2] program. The initial on-axis electric field distribution in the linac cavities (Fig. 6) used in ASTRA simulations was obtained from bead pull measurements. The measured effective length of the electric field in the linac is 0.2215 m. A conflat flange (CF) with titanium foil will be connected to the linac exit, which is 0.06 m downstream the end of the electric field effective length, to separate the vacuum environment and the ambient air. Thus, the interested positions in this study are at the end of the field and at the titanium foil window.

Copyright © 2016 CC-BY-3.0 and by the respective authors

ISBN 978-3-95450-177-9

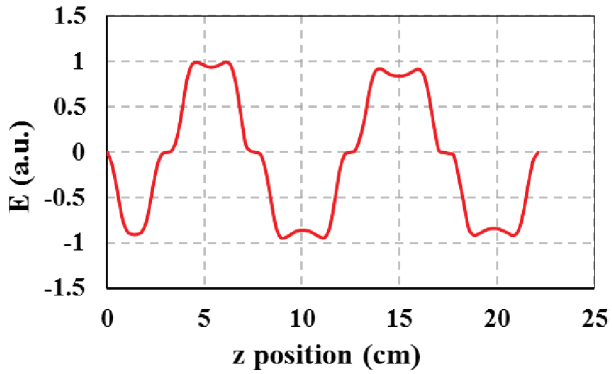

Figure 6: Normalized electric field as a function of longitudinal distance in the linac structure.

In this research, the electron beam energy and current will be varied. In order to vary the beam energy, the peak power of the RF field will practically be adjusted. This results in the different accelerating gradients in the linac structure. Table 2 and Fig. 7 show the results of the output beam energy for four different accelerating gradients. For maximum acceleration, the accelerating gradient of the linac is 41.7 MV/m. This leads to the average kinetic energy of 4.016 MeV and 3.995 MeV at the end of the field and at the titanium window, respectively. A tiny different of the average energy at the two locations can be due to the space charge effect.

Table 2: RF Accelerating gradient (E) and average beam kinetic energy (E_k) at the end of field and at the titanium window

E (MV/m)	E_k at end of field (MeV)	E_k at titanium window (MeV)
16.0	1.032	1.025
20.5	1.962	1.961
29.0	3.028	3.025
41.7	4.016	3.995

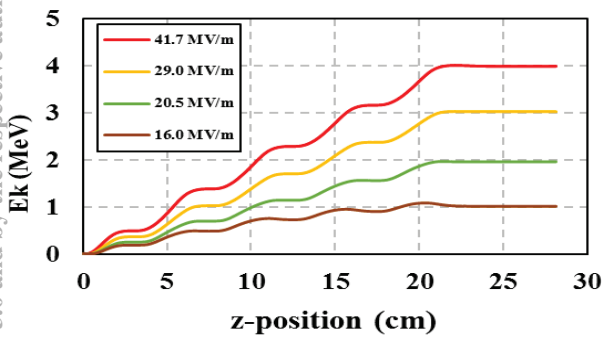

Figure 7: Electron beam kinetic energy as a function of longitudinal (z-position) along the linac structure for four different accelerating gradients.

The simulation results in Fig. 8 show the transverse distributions of electron bunch at the end of field (0.2215 m) and at the titanium window (0.2815 m), respectively. The simulated distributions suggest that the beam diverts with the geometric emittance of 10.15 π mm·mrad at the titanium window. Summary of parameters from ASTRA simulation for the case of maximum acceleration at the end of field and at the titanium window are listed in Table 3.

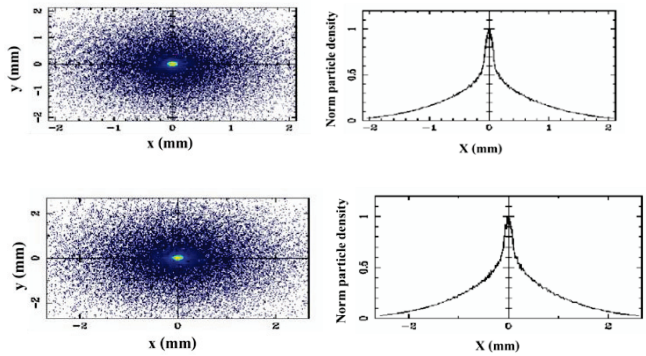

Figure 8: Transverse particle distributions and profiles at the end of field or z = 0.2215 m (top row) and at the titanium window or z = 0.2815 m (bottom row).

Table 3: Results of ASTRA Simulation for the Case of Maximum Acceleration with the Accelerating Gradient of 41.7 MV/m at the end of Field and at the Titanium Window

Parameter	End of field	Titanium window
Average energy	4.016 MeV	3.995 MeV
rms transverse size	0.848 mm	1.070 mm
Bunch charge	300 pC	300pC
rms norm. emittance	9.588 π mm·mrad	10.15 π mm·mrad

DIAGNOSTIC INSTRUMENTS

Design and construction of the electron beam diagnostic instruments of the linac for rubber vulcanization are ongoing. A Faraday cup and an integrated current transformer will be used to measure the electron charge and macropulse current. A dipole magnet, a phosphor screen and a CCD camera will be utilized for an electron beam energy measurement. The transverse beam size and transverse electron distribution at the sample container location will be observed via an in air vacuum screen station.

Charge and Current Measurements

A macropulse current of electron beams produced from this accelerator is measured after the titanium window by using a current transformer (CT) as shown in Fig.9. The current transformer has been designed for the measurement of electron beam with a macropulse width of 4 μs and the current of electron beam can be calculated from

$$I_b = \frac{NV_0}{R}, \quad (2)$$

Copyright © 2016 CC-BY-3.0 and by the respective authors

ISBN 978-3-95450-177-9

where I_b is the current of electron beam, N is the number of wiring turns, V_0 is the voltage across R, and R is the resistant of the load. From the test results, the current transformer has N = 16 and R= 50 Ω. Furthermore, a Faraday cup will be installed downstream the current transformer to measure the electron charge. Both signals from the current transformer and the Faraday cup are observed by a digital oscilloscope.

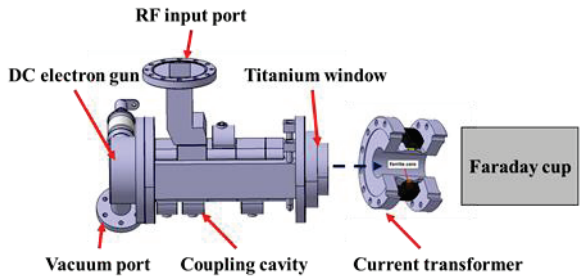

Figure 9: Schematic setup to measure the electron macropulse current and the electron charge.

Energy Measurement

A dipole magnet, a phosphor screen and a CCD camera will be used to measure the electron beam energy after exiting the linac. The energy measurement will be performed in ambient air. The dipole magnet with the magnetic field of 183.63 mT can bend 4 MeV electron beam with a bending angle of 60°. Then, the energy of the electron beam can be calculated from

$$\frac{1}{\rho[\mathrm{m}]} = 0.2998 \frac{\mathrm{ZB_0[T]}}{\beta \mathrm{E[GeV]}} \qquad (3)$$

where ρ is the bending radius, Z is the charge multiplicity, B_0 is the magnetic intensity, E is the electron beam energy in GeV.

The setup of the electron beam energy measurement is shown in Fig. 10. The diameter of the titanium foil window is 5 cm. In this setup, the dipole magnet will be placed as close as possible to the titanium window exit to avoid the loss of the electron beam in air.

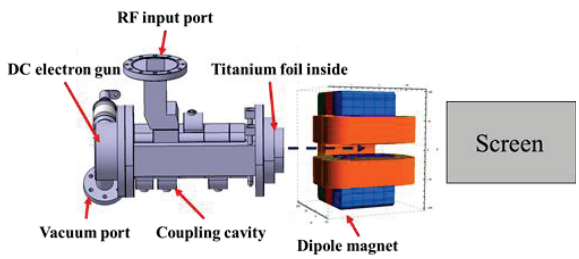

Figure 10: Schematic setup of electron beam energy measurement.

CONCLUSION

In this paper, we present the progress of development on the electron linear accelerator system and beam diagnostic instruments for natural rubber and polymer researches. The high power RF commissioning results show that the resonant frequency of the linac structure is 2997.103 MHz at the operating temperature of 35°C. The maximum RF pulse duration is 4 μs with 200 Hz of pulse repetition rate. This experimental information gives an average RF power of 1.32 kW. From beam dynamic study with the accelerating gradient of 41.7 MV/m, the simulated electron beam average energy at the titanium window is 3.995 MeV. The rms transverse beam size equals to 0.848 mm and 1.070 mm at the end of field and at the titanium window, respectively.

Currently, electron beam diagnostic instruments to measure electron macropulse current, electron charge, beam energy, transverse beam size and transverse beam distribution are under design and construction. The current transformer and the faraday cup will be used to measure the electron beam pulse current and charge. The dipole magnet with screen station has been designed to measure the electron beam energy after passing the titanium window. Furthermore, parameters of electron beams after exiting the titanium window and at the sample irradiation location will be simulated by using the Monte Carlo simulation program GEANT4. [3,4] The beam parameters will be measured to compare with the simulation prediction.

ACKNOWLEDGEMENTS

The authors would like to acknowledge the supports by the Department of Physics and Materials Science, the Faculty of Science, Chiang Mai University, the Science Achievement Scholarship of Thailand, the Thailand Center of Excellence in Physics (ThEP Center) and the Science and Technology Park Chiang Mai University (CMU STeP).

REFERENCES

[1] Gex Corportion; Colorado: Gex Corporation the Dosimetry Company. Available on: [cited 2016 Sep. 06], http://gexcorporation.com/pro-dosimetry-system.php

[2] K. Flottman, ASTRA particle tracking code, http://www.desy.de/mpyflo/.

[3] S. Agostinelli, J. Allison, K. Amako, J. Apostolakis, H. Araujo, P. Arce *et al.,* Nucl. Instrum. Methods A 506 (2003) 250-303.

[4] J. Allison, J. Amako, K. Apostolakis, J. Araujo, H. Dubois, P.A. Asai *et al.*, IEEE Trans. Nuc. Sci. 53 (2006) 270-278.

Copyright © 2016 CC-BY-3.0 and by the respective authors

ISBN 978-3-95450-177-9